sustainability

MDPI

Article

Dynamic Modeling Under Temperature Variations for Sustainable Air Quality Solutions: PM2.5 and Negative Ion Interactions

Paola M. Ortiz-Grisales [1,*,†], Leidy Gutiérrez-León [1,†], Eduardo Duque-Grisales [1,2,†] and Carlos D. Zuluaga-Ríos [3,†]

[1] Department of Electrical Engineering, Engineering Faculty, Institución Universitaria Pascual Bravo, Medellín 050036, Colombia; leidy.gutierrez@pascualbravo.edu.co (L.G.-L.); e.duque@pascualbravo.edu.co (E.D.-G.)
[2] Business Studies Faculty, Institución Universitaria Esumer, Medellín 050036, Colombia
[3] Institute for Research in Technology, Universidad Pontificia Comillas, 280015 Madrid, Spain; czuluaga@comillas.edu
* Correspondence: paola.ortiz@pascualbravo.edu.co
† These authors contributed equally to this work.

Abstract: Air pollution caused by fine particles known as PM2.5 is a significant health concern worldwide, contributing to illnesses like asthma, heart disease, and lung cancer. To address this issue, this study focused on improving air purification systems using negative ions, which can attach to these harmful particles and help remove them from the air. This paper developed a novel mathematical model based on linear differential equations to study how PM2.5 particles interact with negative ions, making it easier to design more effective purification systems. The proposed model was validated in a small, controlled space, using common urban pollutants such as cigarette smoke, incense, coal, and gasoline. These tests were conducted at different temperatures and under two levels of ion generation. The results showed that the system could remove over 99% of PM2.5 particles in five minutes when temperatures were low or moderate. However, at higher temperatures, the system's performance dropped significantly. This research goes beyond earlier studies by examining how temperature affects the process, which had not been fully explored before. Furthermore, this approach aligns with global sustainability goals by promoting public health, reducing healthcare costs, and providing scalable solutions for sustainable urban living.

Keywords: negative ions; PM2.5; air purification; environmental sustainability; air quality; environmental impacts; dynamic modeling; electrostatic recombination; mass conservation; deterministic modeling; ionization efficiency; temperature variation

Academic Editors: Luca Stabile and Maxim A. Dulebenets

Received: 29 October 2024
Revised: 17 December 2024
Accepted: 21 December 2024
Published: 26 December 2024

Citation: Ortiz-Grisales, P.M.; Gutiérrez-León, L.; Duque-Grisales, E.; Zuluaga-Ríos, C.D. Dynamic Modeling Under Temperature Variations for Sustainable Air Quality Solutions: PM2.5 and Negative Ion Interactions. *Sustainability* **2025**, *17*, 70. https://doi.org/10.3390/su17010070

1. Introduction

Air pollution, particularly from fine particulate matter like PM2.5, has escalated into a global health crisis. According to the World Health Organization (WHO) [1], PM2.5 pollution leads to over 4 million premature deaths yearly due to respiratory and cardiovascular diseases, making it one of the leading environmental risk factors worldwide. Recent studies emphasize the critical impact of PM2.5 pollution on global health and economies. In urban areas, PM2.5 concentrations frequently exceed 35 $\mu g/m^3$, well above the WHO's [2] recommended limit of 5 $\mu g/m^3$ [1]. These elevated levels are linked to a 25% increase in cardiovascular disease risk and a 30% rise in respiratory illnesses [3]. Moreover,

the economic burden of PM2.5 pollution is staggering, with healthcare expenditures and productivity losses surpassing USD 5 trillion [3]. Cities such as Delhi and Beijing, often reporting concentrations above 100 $\mu g/m^3$, face recurring public health emergencies, further underscoring the need for effective intervention strategies [4].

These fine particles, characterized by their extremely small size, with a diameter of 2.5 micrometers or less [5], are capable of penetrating deep into the lungs and even entering the bloodstream, causing inflammation, exacerbating asthma, and increasing the risk of conditions like lung cancer and heart disease [6]. In densely populated urban areas, PM2.5 levels can soar far above recommended limits due to traffic, industrial activities, and other emissions, often exceeding safe levels by up to five times [7].

In response to the growing threat of air pollution, particularly fine particulate matter (PM2.5), air purification systems capable of effectively reducing these concentrations have become vital for safeguarding public health and enhancing the quality of life [8,9]. Among the emerging technologies, negative air ion (NAI) systems have demonstrated remarkable potential, with research showing that NAIs can reduce airborne particulate matter by up to 99% in controlled environments [6]. NAI systems can be broadly classified into two categories: unipolar and bipolar [10]. Unipolar systems, which generate only negatively charged ions, are known for their simplicity and cost-effectiveness. However, their performance can be hindered by uneven ion distribution and the potential for electrostatic imbalance over time, which may reduce efficiency. In contrast, bipolar systems produce both negative and positive ions, enabling a balanced ion concentration that is more effective for comprehensive air purification [10]. These systems are particularly adept at neutralizing bacteria, viruses, and volatile organic compounds (VOCs). However, bipolar systems are more complex, expensive, and energy-intensive than their unipolar counterparts.

Despite these challenges, NAI systems represent an innovative and sustainable solution to air pollution, especially in environments where clean air is critical, such as high-traffic areas, schools, hospitals, and workplaces. As PM2.5 pollution continues to pose significant health risks and economic burdens, the urgency for advanced air purification technologies cannot be overstated. According to the World Health Organization [11], addressing PM2.5 is essential to mitigating its far-reaching societal impacts. Investing in effective air purification systems, particularly in urban areas, is not merely an environmental responsibility but a pressing public health priority. By improving air quality, these systems contribute directly to the achievement of Sustainable Development Goals (SDGs), including SDG 3 (Good Health and Well-Being) and SDG 11 (Sustainable Cities and Communities) [3,12]. In an increasingly urbanized world, such innovations are indispensable for protecting human health and ensuring a higher quality of life for all.

Modeling the interaction between PM2.5 and negative ions is crucial for advancing the efficiency of negative ion-based air purification systems. PM2.5 particles, due to their small size and chemical composition, can remain suspended in the air, posing significant health risks when inhaled. By accurately modeling how these particles interact with negative ions, researchers can better understand the mechanisms through which ions attach to or neutralize harmful particles, ultimately facilitating their removal from the air. Extensive research on PM2.5 particulate matter purification using NAIs has led to the development of various modeling approaches to better understand this interaction [13].

In modeling the interaction between PM2.5 and NAIs, studies such as [14] used first-order differential equations and neural networks to capture the relationship between particulate matter concentration and small ions in controlled environments. This approach improved prediction accuracy through accessible measurements but lacked adjustments for environmental variations, limiting its applicability in dynamic, real-world settings. Similarly, Ref. [10] presented a methodology grounded in experimental tests with unipolar

and bipolar ionizers, measuring particle concentration and ozone generation. The study provided experimental support for enhanced filtration and ozone control, although bipolar ionizers demonstrated limited effectiveness in certain controlled environments. Additionally, environmental variability can impact the results, indicating a need for improved robustness across scenarios. In another study, Ref. [13] introduced an experimental method for air purification using negative oxygen ions generated at low voltages with nanometric carbon fibers. Utilizing an exponential model, the device achieved a 96.5% PM2.5 reduction in five minutes, reaching 99.09% in 30 min within a closed space. However, the rapid ion dispersion affected clean air delivery rates, necessitating multiple devices or adjustments to cover larger areas, increasing system complexity and cost. On the other hand, Ref. [15] evaluated the performance of commercial indoor air purification systems for PM2.5 through a linear dynamic model based on mass conservation. The study achieved a 97.9% PM2.5 reduction in 30 min. However, it did not incorporate PM2.5 interactions with other elements or temperature variations, which could impact accuracy and efficacy in real settings.

In a different approach, Ref. [16] proposed a data-based model to examine the relationships between negative ions and environmental factors like humidity, radiation, and temperature in urban parks. While informative, this study was limited to exploring these relationships without a focus on particulate matter reduction, thus reducing its relevance to air purification. Further, Ref. [17] examined the interaction between airborne particles and ions in urban areas with varying vehicular pollution in Brisbane, Australia. Although the empirical methodology differentiated between clean and polluted areas, it faced challenges in generalizing results and balancing measurements of positive and negative ions, complicating broader urban applications. In [18], data-driven models were used to explore the interaction between negative ions and environmental factors, such as particulate matter, humidity, and temperature. Despite handling multiple variables, the study was limited by potential overfitting and dependency on site-specific data, reducing generalizability. In [19], the authors proposed combining variational mode decomposition and gated recurrent neural networks to achieve high precision and adaptability in capturing nonlinear data patterns in air pollution modeling with a focus on particulate matter. However, they did not specifically analyze interactions with negative ions, and the approach required significant computational resources, limiting its practical use. In [20], the authors studied volatile organic compounds (VOCs) adsorption on PM2.5 using mass spectrometry and gas chromatography, showing effective VOC reduction in negative ion-enriched environments. However, the method was limited to specific VOCs and involved high computational costs, reducing its scalability for larger applications. Finally, Ref. [21] used numerical simulation to study particle deposition in air purifier filters through adsorption, assessing dust removal effectiveness. This mass-balance model considered factors like ventilation, chemical transformation, and suspension from human activity. While adsorption filters were effective for larger particles (PM10), they were less effective for ultrafine particles (PM2.5 and smaller), which could pass through or remain suspended, limiting their efficiency in removing the most harmful particles to health.

While various methods exist to model and predict PM2.5 behavior and its interaction with negative ions, many exhibit substantial limitations, such as insufficient consideration of environmental variability, high computational costs, and challenges in generalizing results. These issues underscore the need for more comprehensive and efficient models that address these gaps to enhance the effectiveness of air purification systems using negative ions. This paper presents a linear parametric dynamic approach grounded in the law of mass conservation to model the interaction between PM2.5 particles and negative ions in air purification. We aim to build on the work of [13,15] by jointly addressing the interaction

between PM2.5 and ions. For this purpose, a controlled cubic chamber with dimensions of 40 cm per side was used to study the interaction between negative ions and PM2.5, testing four common urban pollutants (cigarette smoke, incense, coal, and gasoline [22,23]) across two voltage levels (7.5 kV and 30 kV) and three temperature ranges (14–17 °C, 23–27 °C, and 39–51 °C). A total of 36,000 samples were collected by testing each combination of voltage, temperature, and pollutant five times, with measurements recorded every second over 300 s. High-precision devices monitored negative ion and PM2.5 concentrations, as well as temperature, humidity, formaldehyde, and TVOC levels. Through this experimental procedure and the proposed model, the optimal parameters for each experimental condition were estimated. From the optimal modeling performed under controlled conditions, it was found that the proposed model effectively captures both the evolution of particulate matter and the dynamics of negative ions. Experimental results indicate that the proposed study achieves over 99% efficiency within five minutes at low and medium temperatures; however, efficiency declines to 32.66% at high temperatures with 7.5 kV. Additionally, the results show that the model is suitable for changes in the environment, such as temperature. To summarize, the main features and contributions of this study are as follows:

- A novel linear parametric dynamic model, rooted in the law of mass conservation, is introduced to effectively capture and model the interaction dynamics between PM2.5 particles and negative ions.
- A controlled chamber is proposed to study the interactions between negative ions and PM2.5 with various urban pollutants.
- An experimental procedure under controlled conditions, considering temperature variations and two ionization voltages, is proposed.
- Over 99% efficiency is achieved within five minutes at low and medium temperatures in this study.

2. Deterministic Dynamic Modeling vs. Data-Driven Modeling

Modeling the interaction between PM2.5 particles and negative ions is crucial for designing effective air purification systems. Two common approaches, deterministic methods [15,24–26] and data-driven techniques [18,27–29], offer distinct advantages and limitations. Deterministic models, grounded in principles like mass conservation, provide a clear and interpretable framework for understanding the underlying processes, making them ideal when data are limited or expensive to obtain. In contrast, data-driven models rely on extensive, high-quality datasets and often focus on correlations rather than causation, which can obscure the physical mechanisms at play. Given this study's focus on understanding PM2.5 and negative ion interactions under controlled conditions, a deterministic approach was selected. This method enables precise estimation of interaction coefficients and environmental effects, such as temperature variations, while maintaining interpretability and reliability [30]. By addressing gaps in existing research, such as the impact of environmental variability, the deterministic model offers a scalable and cost-effective foundation for developing sustainable air purification systems.

3. Dynamic Approximation of PM2.5 and Negative Ion Interactions

In modeling the interaction between NAIs and PM2.5, we assume a closed and homogeneous system where species are concentrated under controlled conditions. The evolution of PM2.5 and NAIs follows the law of mass conservation [13,15], which maintains that the total mass within the system remains constant [31]. This principle dates back to the 17th-century observations by Dr. Jean Rey, who noted that the weight of matter remains

constant regardless of its form or volume. Building on this foundation, the general mass balance equation for such a system is represented as follows [32]:

$$\frac{dC}{dt} = \text{Generation} - \text{Elimination} - \text{Interaction}, \tag{1}$$

where $\frac{dC}{dt}$ represents the rate of change in the concentration of a species C in a system over time, accounting for three main factors: the generation of the species within the system, its removal, and its interaction with other species present in the system [33]. This mass balance equation is widely used in dynamic system simulations, enabling the modeling of concentration changes over time [15,33]. Applications include quantifying human PM2.5 exposure in various environments [34] and predicting contaminant levels in controlled ventilation systems [35], making it a suitable approach for the proposed system model.

Expanding upon the approach presented in [15], this paper models the interaction between PM2.5 and negative ion concentrations through a linear parametric dynamic approach based on (1). Our mass balance-based model assumes that the temporal dynamics of these interactions in a controlled environment align with the behavior outlined in Equation (1). Accordingly, the rate of change in PM2.5 and ion concentrations is captured by the following equations:

$$\frac{dC_{\text{PM2.5}}}{dt} = G_{\text{PM2.5}} - E_{\text{PM2.5}} \cdot C_{\text{PM2.5}} - k_1 \cdot C_{\text{PM2.5}} \cdot C_{\text{ions}}, \tag{2}$$

$$\frac{dC_{\text{ions}}}{dt} = G_{\text{ions}} - E_{\text{ions}} \cdot C_{\text{ions}} - k_2 \cdot C_{\text{PM2.5}} \cdot C_{\text{ions}}, \tag{3}$$

where $G_{\text{PM2.5}}$ and G_{ions} denote the generation rates of PM2.5 and ions, respectively, which are influenced by external factors such as pollutant sources and ionizer performance. Similarly, $E_{\text{PM2.5}} \cdot C_{\text{PM2.5}}$ and $E_{\text{ions}} \cdot C_{\text{ions}}$ describe the natural removal rates of each species, accounting for processes like sedimentation or dispersion. Interaction coefficients (i.e., k_1 and k_2) quantify the recombination dynamics between PM2.5 and ions, represented mathematically by $k_1 \cdot C_{\text{PM2.5}} \cdot C_{\text{ions}}$ and $k_2 \cdot C_{\text{PM2.5}} \cdot C_{\text{ions}}$, which model the reductions in their concentrations. These coefficients are pivotal in capturing the efficiency of particulate removal under varying conditions. The interaction coefficients are particularly sensitive to environmental factors such as temperature and humidity. Elevated temperatures increase the kinetic energy of particles and ions, enhancing collision frequencies and improving recombination rates. Conversely, higher humidity promotes particle growth by increasing the size and mass of PM2.5 particles, which enhances their likelihood of colliding with ions [36]. From Equations (2) and (3), the reaction terms can be defined as follows:

$$R_{\text{PM2.5}} = k_1 C_{\text{ions}} C_{\text{PM2.5}}, \quad R_{\text{ions}} = k_2 C_{\text{ions}} C_{\text{PM2.5}}. \tag{4}$$

By simplifying (2) and (3), we obtain the following equations:

$$\frac{dC_{\text{PM2.5}}}{dt} = G_{\text{PM2.5}} - E_{\text{PM2.5}} - R_{\text{PM2.5}}, \tag{5}$$

$$\frac{dC_{\text{ions}}}{dt} = G_{\text{ions}} - E_{\text{ions}} - R_{\text{ions}}. \tag{6}$$

From the above, we denote the constants as follows:

$$A = G_{\text{PM2.5}} - E_{\text{PM2.5}}, \quad B = G_{\text{ions}} - E_{\text{ions}}.$$

Under the assumption of proportionality, we can assume that $k_1 = k_2 = k$ and $A = B$. This simplifies (5) and (6) to

$$\frac{dC_{\text{PM2.5}}}{dt} = A - kC_{\text{PM2.5}}C_{\text{ions}}, \tag{7}$$

$$\frac{dC_{\text{ions}}}{dt} = A - kC_{\text{PM2.5}}C_{\text{ions}}. \tag{8}$$

Since (7) and (8) are equivalent under the proportionality assumption, we have

$$C_{\text{PM2.5}} - C_{\text{ions}} = c, \tag{9}$$

where c is a constant. Substituting $C_{\text{ions}} = C_{\text{PM2.5}} - c$ into (7), we obtain the Riccati equation for $C_{\text{PM2.5}}$:

$$\frac{dC_{\text{PM2.5}}}{dt} + kC_{\text{PM2.5}}^2 - kcC_{\text{PM2.5}} = A. \tag{10}$$

By solving Equation (10), we obtain the general solution for $C_{\text{PM2.5}}(t)$:

$$C_{\text{PM2.5}}(t) = C_p + \frac{1}{k\beta} + De^{-\beta t}, \tag{11}$$

where C_p, β, and D are constants determined by the initial conditions. Finally, the solution for $C_{\text{ions}}(t)$ is given by

$$C_{\text{ions}}(t) = C_{\text{PM2.5}}(t) - c. \tag{12}$$

Equations (11) and (12) provide a solution under the assumption of proportionality between the reaction terms, allowing for a representation of the temporal evolution of PM2.5 particles and ion concentrations. This model is an approximation of the interaction between PM2.5 and negative ions across various environmental conditions, capturing the dynamic reduction of particulate matter through ion generation. It serves as a practical tool for both experimental and theoretical applications, improving the understanding of air purification mechanisms in controlled settings. However, the model's assumption of a homogeneous system excludes certain factors, such as spatial and temporal variations; meteorological conditions like wind speed, temperature, and humidity [37]; and equipment limitations affecting measurement accuracy [38,39]. Furthermore, the model does not incorporate the effects of humidity and temperature on ionization efficiency, which may influence the recombination process with PM2.5 particles [40,41]. Including these factors, as well as other pollutants and environmental fluctuations, would enhance the model's applicability to real-world conditions.

4. Experimental Setup

The experiments took place from March to August 2024 in a controlled cubic chamber (see figure 1) with dimensions of 40 cm per side to evaluate the interaction between negative ions and particulate matter (PM2.5) in Medellín, Colombia [42]. Four common urban pollutants were used (cigarette smoke, incense, coal, and gasoline [22,23]) under two voltage levels (7500 V and 30,000 V) and three temperature ranges: low (14–17 °C), medium (23–27 °C), and high (39–51 °C). The voltage level of 30 kV refers to a modular setup of four devices, each with a 7.5 kV booster, combining to achieve 30 kV for ion generation and optimizing air purification efficiency in the experiment.

The initial PM2.5 concentration was defined at 1000 µg/m³ due to the measurement range and capabilities of the DM306 portable air quality monitor. This concentration was achieved by introducing a controlled amount of pollutants into the test chamber. Once introduced, the pollutants were allowed to disperse naturally, ensuring uniform

distribution throughout the chamber. To confirm the accuracy and consistency of the PM2.5 concentration, multiple measurements were taken and cross-verified using a secondary air quality monitor DT-9881, which features a broader measurement range of up to 2000 µg/m³. This validation ensured the reliability of the experimental setup. Elevated concentrations of pollutants were selected to generate a representative response curve, allowing for a robust evaluation of the interaction between negative ions and particulate matter under controlled conditions [42]. Following the procedure described above, a preliminary set of experiments was conducted without activating the negative ion generation system, as illustrated in Figure 2. The figure demonstrates that, in the absence of ionization, PM2.5 concentrations exhibit minimal fluctuations around an average value, with no discernible trend toward reduction. This approach establishes a baseline and provides a better understanding of the natural behavior of particles within the chamber.

(**a**) The controlled test cabinet. (**b**) Measurement equipment.

Figure 1. Experimental conditions.

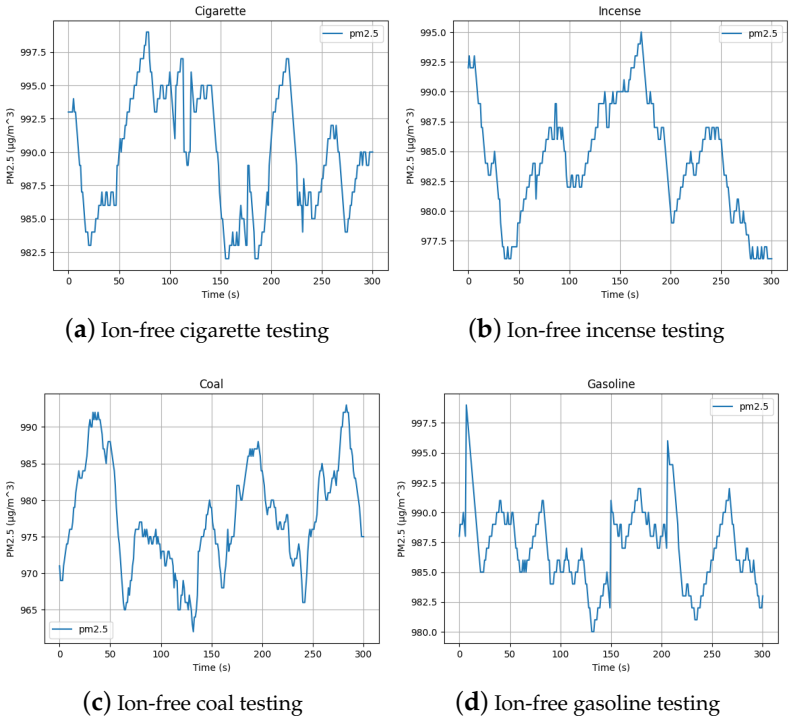

(**a**) Ion-free cigarette testing (**b**) Ion-free incense testing

(**c**) Ion-free coal testing (**d**) Ion-free gasoline testing

Figure 2. PM2.5 behavior in ion-free environments.

Each combination of voltage, temperature, and pollutant was repeated five times, resulting in a total of 36,000 samples. Measurements were taken every second for 300 s, recording data on PM2.5 reduction under various conditions. The negative ion generation

system used a high-voltage circuit, with ion concentrations measured by the KT-401 aerosol ion tester, which operates by detecting the electrical charge of ions present in the chamber air. PM2.5, temperature, relative humidity, formaldehyde, and total volatile organic compounds (TVOCs) were monitored by the DM306. From the experimental data, precise measurements of negative ion and PM2.5 concentrations over time were obtained. Figures 3 and 4 display the results for the selected pollutants, reflecting the concentration trends across different temperatures and voltages. The data are available in the open science framework repository [42]. In Figure 3, three experimental tests are depicted, showing the behavior of particulate matter as it interacts with negative ions in the test chamber. Three temperature ranges were analyzed, with varying quantities of negative ions introduced to examine their impact on particle sedimentation via electrostatic recombination. Notably, a rapid decline in ion concentration was observed within the first seconds of the experiments, driven by high recombination rates between ions and PM2.5 particles. This immediate interaction, triggered by the activation of the ion generation system, resulted in swift recombination as the ions bonded with the particulate matter. Figure 3 reveals a clear trend, indicating that increasing the ion generation voltage beyond 30,000 V has the potential to further enhance the rate of particulate matter removal. However, practical considerations, such as ozone generation and energy consumption, must be addressed. Additionally, the combined effects of high humidity and elevated voltage could enhance particle growth, further promoting sedimentation. These findings underscore the importance of optimizing both voltage and environmental parameters to ensure the model's applicability across diverse real-world scenarios [42]. Conversely, reducing ionization voltage below 7.5 kV may significantly extend the time required to purify the air. Lower ion production and weaker electric fields decrease the frequency of ion–particle collisions, thereby slowing recombination rates and particle sedimentation [13].

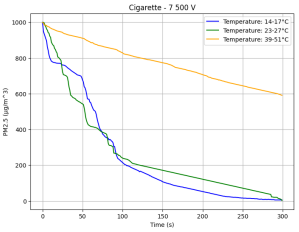

(**a**) Cigarette smoke with ion generation at 7500 V.

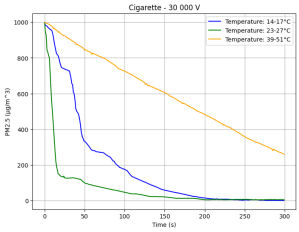

(**b**) Cigarette smoke with ion generation at 30,000 V.

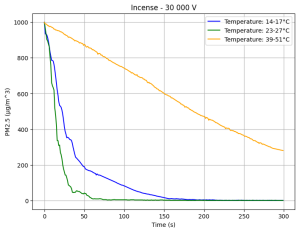

(**c**) Incense smoke with ion generation at 30,000 V.

Figure 3. Behavior of PM2.5 concentrations under different ion generation voltages and three temperature levels.

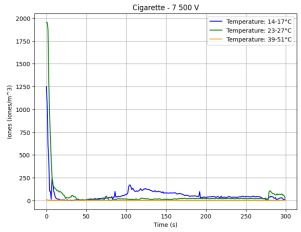

(**a**) Ion concentration at 7500 V with cigarette smoke.

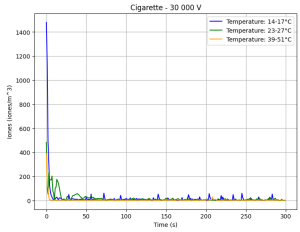

(**b**) Ion concentration at 30,000 V with cigarette smoke.

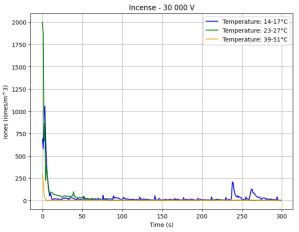

(**c**) Ion concentration at 30,000 V with incense smoke.

Figure 4. Behavior of negative ions when interacting with pollutants under three temperature levels.

Figure 4 presents three experimental tests illustrating the behavior of negative ions in the experimental space as they interact with particulate matter. The quantity of negative

ions was adjusted to analyze how they influence the distribution and dispersion of particles in the environment.

5. Proposed Modeling Framework

Following the presentation of the experimental data collected under controlled conditions, as outlined in Section 4, and the formulation of the deterministic model based on the solutions of (11) and (12), it becomes essential to estimate the parameter values associated with these equations. This estimation aims to align the model's response with the observed experimental results. Parameter estimation for the proposed model was achieved by solving an optimization problem aimed at minimizing the discrepancy between the model's response and the actual observed interactions between PM2.5 and negative ions, as described in [43]. The optimization problem is given as follows:

$$\min_{\boldsymbol{\theta}} f(\boldsymbol{\theta}) \tag{13}$$

subject to

$$\boldsymbol{\theta}_{\min} \leq \boldsymbol{\theta} \leq \boldsymbol{\theta}_{\max}, \quad \boldsymbol{\theta} \in \mathbb{R}, \tag{14}$$

where $\boldsymbol{\theta} = [G_{\text{PM2.5}}, E_{\text{PM2.5}}, G_{\text{ions}}, E_{\text{ions}}, k_1, k_2]^\top$, $\boldsymbol{\theta}_{\min}$ y $\boldsymbol{\theta}_{\max}$ corresponds to the set of minimum and maximum values that the parameters can reach within the search space, respectively. On the other hand, $f(\boldsymbol{\theta})$ is defined as the Root Mean Square Error (RMSE) between the model responses based on (2) and (3) and the experimental results for the concentrations of PM2.5 and negative ions. This objective function is calculated as follows:

$$f(\boldsymbol{\theta}) = \frac{1}{n}\sum_{i=1}^{n}\left(\tilde{C}_{\text{PM2.5}_i}(\boldsymbol{\theta}) - C_{\text{PM2.5}_i}(\boldsymbol{\theta})\right)^2 + \frac{1}{n}\sum_{i=1}^{n}\left(\tilde{C}_{\text{ions}_i}(\boldsymbol{\theta}) - C_{\text{ions}_i}(\boldsymbol{\theta})\right)^2, \tag{15}$$

where $\tilde{C}_{\text{PM2.5}}(i)$ and $\tilde{C}_{\text{ions}}(i)$ are the predicted concentrations for PM2.5 and negative ions over time i, $C_{\text{PM2.5}}(i)_{\text{obs}}$ and $C_{\text{ions}}(i)_{\text{obs}}$ are the experimentally observed concentrations, and n is the total number of experimental data points. To solve the optimization problem outlined in (13), the differential evolution method, detailed in (16), was employed to estimate the model's optimal parameters. Ultimately, the objective function was designed to minimize the RMSE, as described in (15). This solution method operates by generating multiple candidate vectors $\boldsymbol{\theta}$ or possible solutions, mutating them, and selecting the best parameter combinations in each iteration [44]. Differential evolution is represented by the following expression:

$$\boldsymbol{\theta}_{\text{new}} = \boldsymbol{\theta}_{\text{best}} + \alpha(\boldsymbol{\theta}_{\text{rand1}} - \boldsymbol{\theta}_{\text{rand2}}) \tag{16}$$

where $\boldsymbol{\theta}_{\text{new}}$ is the new parameter vector solution, $\boldsymbol{\theta}_{\text{best}}$ is the current best parameter vector solution, $\boldsymbol{\theta}_{\text{rand1}}$ and $\boldsymbol{\theta}_{\text{rand2}}$ are two randomly selected vectors from the population, and $\boldsymbol{\alpha}$ is the scale factor that controls the magnitude of the mutation. Differential evolution is commonly applied in particulate matter research for its effectiveness in navigating nonlinear, non-differentiable solution spaces [44]. Studies by Teng et al. [45] and Rubal and Kumar [46] highlight its role in enhancing predictive accuracy for air particle concentrations and atmospheric pollutants by optimizing solution parameters. Throughout the optimization, the parameters that best aligned the model with the experimental data were selected. This proposed modeling framework is summarized in Figure 5.

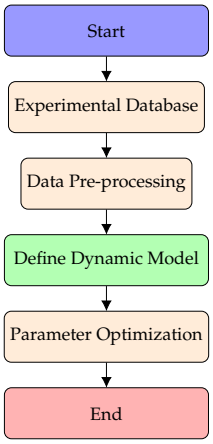

Figure 5. Flowchart for the proposed modeling framework for the dynamic approximation of interactions between PM2.5 and negative ions.

Validation Metrics

To quantitatively assess the performance of the air purification system, the efficiency was calculated following the method described by [13], which is given by

$$\text{Efficiency} = \frac{C_{(i)\text{PM2.5}} - C_{(f)\text{PM2.5}}}{C_{(i)\text{PM2.5}}} \times 100, \tag{17}$$

where $C_{(i)\text{PM2.5}}$ is the initial concentration of PM2.5 and $C_{(f)\text{PM2.5}}$ is the final concentration at the end of the experiment. The efficiency after 5 min and the time to reach 95% were determined by measuring the initial and final PM2.5 concentrations in each experiment, following the method in (17). The time was only recorded when 95% efficiency was achieved.

Additionally, the Pearson correlation coefficient was calculated to evaluate the relationship between the optimal system parameters obtained by the optimization algorithm. This matrix was obtained using the general formula for correlation between two variables X and Y:

$$r_{X,Y} = \frac{\frac{1}{n}\sum_{i=1}^{n}\left(X_i - \overline{X}\right)\left(Y_i - \overline{Y}\right)}{\sqrt{\frac{1}{n}\sum_{i=1}^{n}\left(X_i - \overline{X}\right)^2}\sqrt{\frac{1}{n}\sum_{i=1}^{n}\left(Y_i - \overline{Y}\right)^2}}, \tag{18}$$

where X and Y represent any pair of experimental parameters, such as $G_{\text{PM2.5}}$ and $E_{\text{PM2.5}}$, or G_{ions} and E_{ions}. X_i and Y_i are the individual values of X and Y in each observation, while $\overline{X}$ and $\overline{Y}$ are the means of X and Y, respectively. Finally, n is the total number of observations.

6. Results and Discussion

After discussing the proposed methodology to model the interaction between PM2.5 and negative ions, the air purification system's performance was assessed using Equation (17), with the results presented in Table 1. This table presents the efficiency metrics of the air purification system under varying temperature ranges and ion generation voltage levels. Two primary efficiency indicators were assessed: the total system efficiency at the end of the experiment and the time taken to reach a 95% efficiency level.

Table 1. Comparison of the efficiency achieved at the end of the experiment (5 min) and the time required to reach 95% system efficiency across different temperature ranges.

Ion Generation	Temperature Range	Efficiency at 5 min.	Time to 95% Efficiency
7.5 kV	Low	99.08 %	3.5 min.
7.5 kV	Medium	99.78 %	3.1 min.
7.5 kV	High	32.66 %	-
30 kV	Low	98.29 %	3.0 min.
30 kV	Medium	99.64 %	2.1 min.
30 kV	High	82.83 %	-

In contrast to the findings by [13], where a 2.16 kV negative oxygen ion source with nanometer-scale carbon fibers achieved 96.5% efficiency in five minutes and 99.09% in 30 min within a closed environment, our air purification system operated at higher ionization voltages under controlled temperature conditions. At 7.5 kV, the system achieved an average total efficiency of 99.08% under low temperatures, reaching 95% efficiency in 3.5 min. Under medium temperature conditions, the total efficiency increased to 99.78%, with 95% reached in 3.1 min. However, at high temperatures, the system's efficiency averaged 32.66%, failing to reach 95%. At 30 kV, the system demonstrated a total efficiency of 98.29% at low temperatures, reaching 95% efficiency in 3.0 min. Medium temperature conditions further improved the total efficiency to 99.64%, achieving 95% within 2.1 min. At high temperatures, the system's efficiency averaged 82.83%, also without reaching 95%. These results reveal significant variability in purification efficiency as a function of temperature and ionization voltage.

The effectiveness of ionic air purification systems is influenced by several environmental and operational factors [47]. Freestream air velocity (FAV) plays a significant role, as lower FAV improves the deposition of smaller particles, consistent with the temperature-dependent findings. Relative humidity also enhances particle aggregation and recombination efficiency by increasing particle size and weight [48,49]. Additionally, the physical properties of surrounding surfaces, such as roughness, dielectric constant, and electrical resistivity, affect airflow and particle deposition rates [50]. Turbulence intensity further influences these outcomes, with lower turbulence promoting ion stability and improving deposition efficiency [51]. To maximize the performance of ionic air purifiers, it is essential to optimize these environmental and operational conditions.

Once the performance of the air purifier was discussed, the optimal parameters of the proposed model were obtained for each of the realizations of the experiment explained in Section 4. For this purpose, $\boldsymbol{\theta}_{\min}$ and $\boldsymbol{\theta}_{\max}$ were defined. For $G_{\text{PM2.5}}$, a range between 0 and 2 was set, reflecting the maximum observed PM2.5 generation rate. The PM2.5 elimination parameter was limited to a range between 0 and 0.04. For the ion generation rate G_{ions}, a range of 0 to 25 was defined. k_1 and k_2 were limited to ranges between 0 and 0.01 and 0 and 0.01, respectively. Based on the above analysis and by solving the optimization problem defined by expressions (13) and (14), Table 2 presents the optimal parameter values obtained from the experimental data analysis for some contaminants and environmental conditions.

Table 2. Optimized parameters and RMSE values for different pollutants under varying conditions. The units of measurement are given as follows: Temp. (°C); Volt. (kV); $G_{PM2.5}$, $E_{PM2.5}$ (μg/m^{3}s); G_{ions}, E_{ions} (ions/cm^{3}s); k_1 (sm^3/ions); k_2 (sm^3/μg); $RMSE_{PM2.5}$ (μg/m^3); and $RMSE_{ions}$ (ions/cm^3).

Pollutant	Temp.	Volt.	$G_{PM2.5}$	$E_{PM2.5}$	G_{ions}	E_{ions}	k_1	k_2	$RMSE_{PM2.5}$	$RMSE_{ions}$
Cigarette Smoke	Low	7.5	0.0176	0.0082	49.85	0.8835	3.025×10^{-4}	1.000×10^{-2}	31.65	78.46
Coal	Mid	7.5	0.0015	0.0184	9.082	0.2941	3.006×10^{-6}	1.433×10^{-6}	24.87	45.26
Gasoline	High	7.5	10	0.0117	0.1731	0.6965	9.343×10^{-5}	2.190×10^{-3}	13.89	97.72
Cigarette Smoke	Low	30	0.0011	0.0067	48.32	0.6626	2.397×10^{-4}	9.668×10^{-3}	82.41	152.41
Coal	Mid	30	0.2622	0.0185	4.9900	0.2142	1.763×10^{-5}	1.092×10^{-5}	22.29	68.74
Incense Smoke	High	30	2.298	0.0029	11.79	0.6704	4.721×10^{-5}	3.557×10^{-3}	4.68	114.38

Table 2 reveals that under high-temperature conditions, the interaction constants k_1 and k_2 were elevated, suggesting increased recombination rates between PM2.5 and ions. This increase aligns with the theoretical model, as higher temperatures boost particle kinetic energy, reducing sedimentation and enhancing suspension [52]. Furthermore, the generation rate of ions, G_{ions}, consistently surpassed $G_{PM2.5}$, reflecting the system's active ion production to ensure sufficient recombination with PM2.5. Meanwhile, $G_{PM2.5}$ remained low, fitting its role as a pollutant. On the other hand, the elimination rate E_{ions} was also notably higher than $E_{PM2.5}$, indicating rapid ion turnover and the need for constant ion generation, while $E_{PM2.5}$ was lower, reflecting a reliance on ion interaction for removal. Finally, this table also shows that the RMSE value for PM2.5 was lower than that for ions, suggesting a closer fit of the model to the experimental data for PM2.5 concentrations than for ion concentrations. This discrepancy is attributed to greater variability in ion dynamics, which are more sensitive to environmental factors such as voltage fluctuations and temperature changes. The model demonstrated varying accuracies under different environmental conditions, as reflected in the RMSE values for the PM2.5 and ion concentrations. At low temperatures and 7.5 kV, the RMSE for PM2.5 was 31.65 μg/m³, and for ions, it was 78.46 ions/cm³. These values indicate reasonable precision for PM2.5. At high temperatures and 30 kV, the RMSE for PM2.5 decreased to 4.68 μg/m³, showing improved precision for particle concentration predictions. In contrast, the RMSE for ions increased to 114.38 ions/cm³, reflecting reduced precision in predicting ion dynamics. This divergence highlights the model's sensitivity to specific factors. PM2.5 predictions benefit from more stable particle behavior at high temperatures. However, ion predictions are affected by greater variability due to environmental and operational conditions. Using the data in Table 2, the behavior of the PM2.5 and negative ion concentrations was derived, as shown in Figure 6.

Figure 6 displays six comparative graphs that illustrate the temporal behavior of the negative ion and PM2.5 concentrations predicted by the proposed model alongside the experimental data, with variations between contaminants, temperature ranges, and voltage levels. Figure 6a–c show the temporal evolution of the PM2.5 concentration, highlighting the close alignment between the experimental observations and model predictions. These subplots confirm that Equation (11), which describes the temporal behavior of $C_{PM2.5(t)}$, effectively captures the progressive decrease in the particle concentration over time. This trend is consistent with the exponential decay model proposed by [13]. In contrast, Figure 6d–f show the response of the negative ion concentration, whose decreasing behavior follows a pattern similar to that of PM2.5. This analysis reveals a direct dependence between the two concentrations, enabling a comparison between the experimentally measured and model-predicted negative ions. The model effectively predicted the initial decrease in the negative ion concentration, consistent with ion–ion recombination, where oppositely charged particles neutralize quickly. However, the experimental data show oscillations not captured by the model, likely due to turbulence or particle re-entries affecting PM2.5

dispersion. These fluctuations may also be the result of variations in pollutant composition, agglomeration, and environmental conditions, such as temperature and humidity [53,54], which influence particle settling and electrostatic recombination. These findings underscore the need to extend the model to address real-world complexities. Experimental conditions provide a foundation for understanding PM2.5 and negative ion interactions. However, real scenarios involve multifactorial influences, such as fluctuating temperatures and humidity, external pollutant sources, and variable airflow. Integrating probabilistic approaches to account for environmental variability is essential.

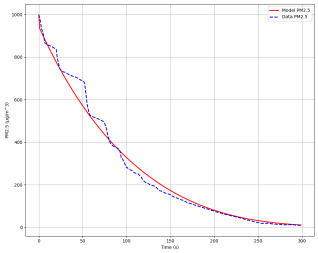

(a) PM2.5 for cigarette smoke at 7.5 kV (low range)

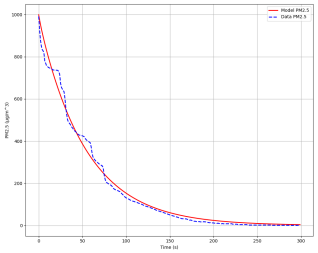

(b) PM2.5 for coal at 7.5 kV (mid-range)

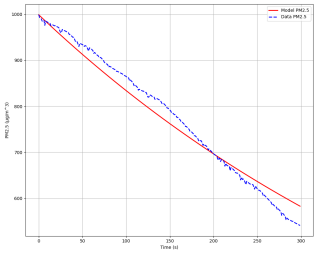

(c) PM2.5 for incense smoke at 30 kV (high range)

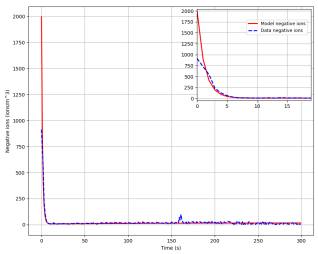

(d) Ions over 300 s (main graph) and the first 20 s (detail) for cigarette smoke at 7.5 kV.

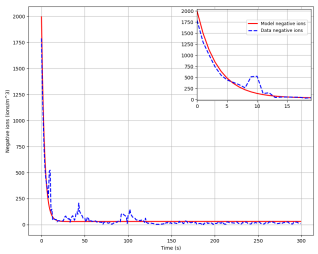

(e) Ions over 300 s (main graph) and the first 20 s (detail) for coal at 7.5 kV.

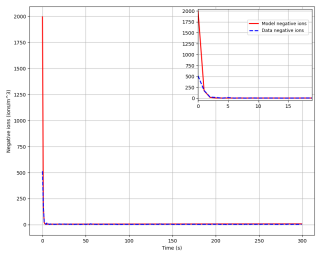

(f) Ions over 300 s (main graph) and the first 20 s (detail) for incense smoke at 30 kV.

Figure 6. Comparison of experimental data and model results for PM2.5 and negative ion interactions.

Global Sensitivity Analysis Using Sobol Indices

The previous section, particularly Figure 6, underscores the effectiveness of the proposed model in capturing the exponential decay of PM2.5 concentrations over time. However, discrepancies such as fluctuations in negative ion concentrations, likely influenced by environmental factors such as turbulence and contaminant composition [53,54], reveal areas for refinement of the proposed model. These observations highlight the importance of sensitivity analysis in identifying the parameters that most influence the dynamics of the system, as described below. The global sensitivity analysis was conducted using Sobol indices to evaluate the relative importance of the parameters involved in the system's dynamics [55]. This approach allowed for the identification of the factors influencing the concentrations of PM2.5 and negative ions over time, as defined in Equations (2) and (3).

The sensitivity analysis categorized parameters based on their Sobol sensitivity indices, following the criteria outlined by Garcia et al. [56]. Parameters with indices above 0.8 were classified as highly relevant, as they significantly influence the system's output variability. Those with indices between 0.5 and 0.8 were considered relevant, indicating secondary but still significant effects. Parameters with indices between 0.3 and 0.5 were deemed marginally relevant, contributing only minimally to the overall variability. To ensure comprehensive coverage of possible parameter values, the Saltelli method was employed for sampling the parameter space [57]. This method used 1000 samples, enabling the estimation of both first-order and second-order interactions between parameters. The bounds for these parameters were derived from the experimental data to reflect realistic

variability. These results were used to calculate both first-order (S_1) and total-order (S_T) Sobol indices.

Figure 7 shows that the elimination terms for the PM2.5 ($E_{PM2.5}$) and ion (E_{ions}) concentrations are highly relevant within the model presented in Equations (2) and (3). These terms consistently exhibit the highest first-order and total-order variances, underscoring their critical influence on system dynamics. Additionally, the generation rate of ions (G_{ions}) is also identified as a significant parameter, as highlighted in the bar plots. The use of Sobol indices enabled a detailed assessment of the relative importance of these parameters in influencing the dynamics of PM2.5 and ion concentrations over time. This sensitivity analysis provides actionable insights for optimizing the air purification system. The results highlight the dominant influence of elimination rates, particularly $E_{PM2.5}$ and E_{ions}, which exhibit the highest sensitivity indices. Precise control over these parameters could significantly enhance system stability under diverse environmental conditions.

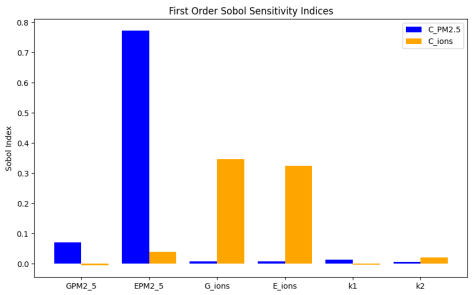

(**a**) First-order Sobol indices for PM2.5 and ions at $t_{eval} = 300$ s.

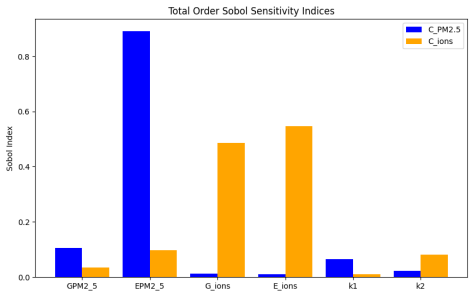

(**b**) Total-order Sobol indices for PM2.5 and ions at $t_{eval} = 300$ s.

Figure 7. First- and total-order Sobol sensitivity indices for PM2.5 and ion concentrations at $t_{eval} = 300$ s.

After analyzing the most relevant parameters in modeling the interaction between PM2.5 and negative ions, we proceeded with a more detailed analysis of these parameters over the course of the experiment. For this analysis, scatter plots between parameters and individual histograms were employed, allowing us to observe each parameter's probability distribution and their interrelations. Figure 8 presents these graphs in matrix form, where the diagonal plots display a histogram for each parameter, while the off-diagonal elements show a scatter plot for each pair of parameters.

In the scatter plots in Figure 8, each subfigure includes a regression line that helps identify the general trend of the relationship between the two variables analyzed [58]. These lines were obtained using Pearson's correlation coefficient, as shown in Equation (18), with the corresponding values presented in Table 3. In Figure 8, the histograms on the diagonal show the operating ranges of each parameter for each of the experiments. The patterns observed in these histograms align with the parameter behaviors presented earlier in Table 2. Next, for each of the histograms, different probability distributions were tested to find the best distribution that fits the behavior of the parameters, represented by the red lines above the histograms. The best-fitting distributions are as follows: $E_{PM2.5}$, which follows a beta distribution; G_{ions} and E_{ions}, which follow a log-normal distribution; and $G_{PM2.5}$, k_1, and k_2, which follow a Weibull distribution, with values concentrated in lower ranges.

Table 3 shows correlations ranging from weak to moderate between variables. For instance, $G_{PM2.5}$ and k_2 exhibit a moderate positive correlation of 0.384, while $E_{PM2.5}$ and k_2 exhibit a negative correlation of -0.441, suggesting an inverse association between these parameters. Most of the Pearson correlations are weak. On the other hand, k_1 and k_2 exhibit a positive correlation of 0.474, showing a moderate relationship. Finally, an inverse relationship is observed between particulate matter PM2.5 and negative ions. This behavior

aligns with the theoretical model, where the generation of negative ions contributes to the removal of particulate matter through electrostatic recombination [29].

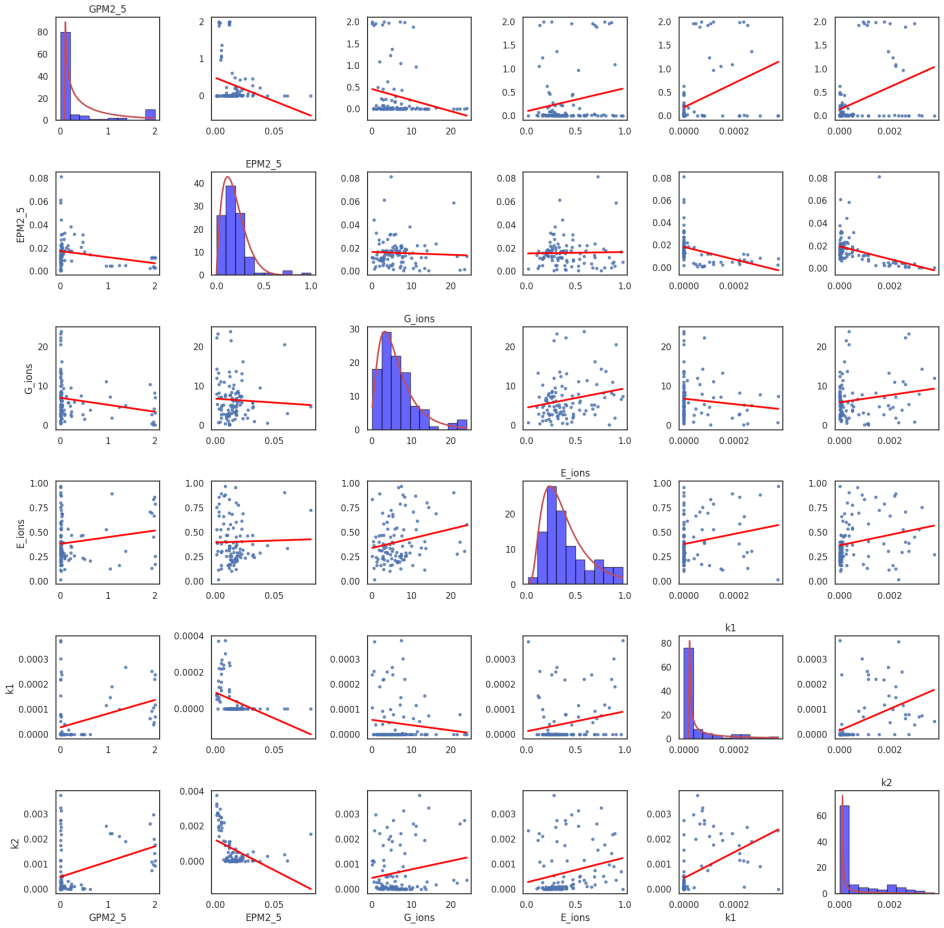

Figure 8. Scatter plots, regression lines and histograms for $G_{PM2.5}$, $E_{PM2.5}$, G_{ions}, E_{ions}, k_1, and k_2. The red lines are regression lines that help identify the general trend of the relationship between the two variables analyzed. The dots represent the relationship between two variables.

Table 3. Pearson correlation coefficients for $G_{PM2.5}$, $E_{PM2.5}$, G_{ions}, E_{ions}, k_1, and k_2.

	$G_{PM2.5}$	$E_{PM2.5}$	G_{ions}	E_{ions}	k_1	k_2
$G_{PM2.5}$	1.000	−0.257	−0.212	0.183	0.377	0.384
$E_{PM2.5}$	−0.257	1.000	−0.049	0.022	−0.398	−0.441
G_{ions}	−0.212	−0.049	1.000	0.218	−0.121	0.178
E_{ions}	0.183	0.022	0.218	1.000	0.204	0.232
k_1	0.377	−0.398	−0.121	0.204	1.000	0.474
k_2	0.384	−0.441	0.178	0.232	0.474	1.000

7. Conclusions

This paper introduced a linear parametric dynamic approach grounded in the law of mass conservation to model the interactions between particulate matter and negative ions, offering a fast, low-cost alternative when experimental data are limited, costly, or time-consuming, and ensuring reproducible results in stable, controlled environments. The optimal parameters were identified to reduce discrepancies between the model and experimental data, revealing that these parameters follow log-normal, beta, and Weibull distributions. This enables uncertainty capture and simulations that enhance system behavior representation under varying conditions. Finally, the proposed air purification system achieved over 99% efficiency within 5 min at low to medium

temperatures using negative ions, outperforming other methods. However, efficiency dropped significantly at higher temperatures, reaching only 32.66% at 7.5 kV. While the experimental conditions provide a robust foundation for understanding the system's behavior, additional adjustments may be required to extend the model's applicability to dynamic, real-world scenarios. These scenarios often involve multifactorial influences, such as the combined effects of fluctuating temperatures and humidity, interactions with external pollutant sources, and varying airflow dynamics. Future work will focus on probabilistic studies that account for environmental variations to predict system performance in various scenarios and recommend experiments at temperatures below 16 °C to assess how reduced particle kinetic energy and increased fluid viscosity affect sedimentation and efficiency. Additionally, it is suggested that effects such as airflow losses, chemical interactions, and experimental validation in heterogeneous environments be incorporated to address real-world complexities. Stochastic approaches could further enhance the model's robustness by quantifying the impact of diverse environmental factors. More complex models are suggested to analyze ion interactions with particulate matter in uncontrolled environments for a more realistic understanding of system effects.

Author Contributions: Conceptualization, methodology, validation, formal analysis, investigation, resources, data curation, writing—original draft preparation, visualization, and final version of the manuscript, P.M.O.-G., L.G.-L., E.D.-G. and C.D.Z.-R. All authors have read and agreed to the published version of the manuscript.

Funding: This research was funded by the Institución Universitaria Pascual Bravo and was derived from the research project titled "Modeling the Air Purification System Using Negative Ions with a Structure for Capturing Particulate Matter Employing Computational Intelligence Methods", under grant number PCT00004.

Institutional Review Board Statement: Not applicable for studies not involving humans or animals

Informed Consent Statement: Not applicable

Data Availability Statement: The original contributions presented in the study are included in the article. Further inquiries can be directed to the corresponding author.

Conflicts of Interest: The authors declare no conflicts of interest.

References

1. World Health Organization. Ambient (Outdoor) Air Pollution. 2024. Available online: https://www.who.int/news-room/fact-sheets/detail/ambient-(outdoor)-air-quality-and-health (accessed on 26 October 2024).
2. de la Salud, O.M. Directrices Mundiales de la OMS Sobre la Calidad del Aire. ISBN 978-92-4-003546-1 (Versión Electrónica) ISBN 978-92-4-003547-8 (Versión Impresa). 2021. Available online: https://iris.who.int/bitstream/handle/10665/346062/9789240035461-spa.pdf (accessed on 24 December 2024).
3. Yin, H.; McDuffie, E.E.; Martin, R.V.; Brauer, M. Global health costs of ambient PM2.5 from combustion sources: A modelling study supporting air pollution control strategies. *Lancet Planet. Health* **2024**, *8*, e476–e488. [CrossRef]
4. Gu, J. The Situation and Prediction of Air PM2.5 Pollution in Shanghai. *Highlights Sci. Eng. Technol.* **2024**, *107*, 104–109. [CrossRef]
5. The U.S. Environmental Protection Agency. Particulate Matter (PM) Basics. 2024. Available online: https://www.epa.gov/pm-pollution/particulate-matter-pm-basics (accessed on 29 November 2024).
6. Jiang, S.; Ma, A.; Ramachandran, S. Negative Air Ions and Their Effects on Human Health and Air Quality Improvement. *Int. J. Mol. Sci.* **2018**, *19*, 2966. [CrossRef]
7. Gifford, F.A. Atmospheric Dispersion Models for Environmental Pollution Applications. In *Lectures on Air Pollution and Environmental Impact Analyses*; American Meteorological Society: Boston, MA, USA, 1982; pp. 35–58. [CrossRef]
8. Yue, C.; Yuxin, Z.; Nan, Z.; Dongyou, Z.; Jiangning, Y. An inversion model for estimating the negative air ion concentration using MODIS images of the Daxing'anling region. *PLoS ONE* **2020**, *15*, e0242554. [CrossRef]
9. Luo, L.; Sun, W.; Han, Y.; Zhang, W.; Liu, C.; Yin, S. Importance Evaluation Based on Random Forest Algorithms: Insights into the Relationship between Negative Air Ions Variability and Environmental Factors in Urban Green Spaces. *Atmosphere* **2020**, *11*, 706. [CrossRef]

10. Romay, F.J.; Ou, Q.; Pui, D.Y.H. Effect of Ionizers on Indoor Air Quality and Performance of Air Cleaning Systems. *Aerosol Air Qual. Res.* **2024**, *24*, 230240. [CrossRef]
11. World Health Organization. *Ambient Air Pollution: A Global Assessment of Exposure and Burden of Disease*; World Health Organization: Geneva, Switzerland, 2016.
12. United Nations Environment Programme (UNEP). *Towards a Pollution-Free Planet: Background Report*; United Nations Environment Programme: Nairobi, Kenya, 2018.
13. Weng, H.; Zhang, Y.; Huang, X.; Liu, X.; Tang, Y.; Yuan, H.; Xu, Y.; Li, K.; Zhang, Y. Pilot Study on the Production of Negative Oxygen Ions Based on Lower Voltage Ionization Method and Application in Air Purification. *Atmosphere* **2024**, *15*, 860. [CrossRef]
14. Davidović, M.; Davidović, M.; Jovanović, R.; Kolarž, P.; Jovašević-Stojanović, M.; Ristovski, Z. Modeling Indoor Particulate Matter and Small Ion Concentration Relationship—A Comparison of a Balance Equation Approach and Data Driven Approach. *Appl. Sci.* **2020**, *10*, 5939. [CrossRef]
15. Shiue, A.; Hu, S.C.; Tseng, C.H.; Kuo, E.H.; Liu, C.Y.; Hou, C.T.; Yu, T. Verification of air cleaner on-site modeling for PM 2.5 and TVOC purification in a full-scale indoor air quality laboratory. *Atmos. Pollut. Res.* **2018**, *10*, 209–218. [CrossRef]
16. Miao, S.; Zhang, X.; Han, Y.; Sun, W.H.; Liu, C.; Yin, S. Random Forest Algorithm for the Relationship between Negative Air Ions and Environmental Factors in an Urban Park. *Atmosphere* **2018**, *9*, 463. [CrossRef]
17. Ling, X.; Jayaratne, R.; Morawska, L. The relationship between airborne small ions and particles in urban environments. *Atmos. Environ.* **2013**, *79*, 1–6. [CrossRef]
18. Shi, G.Y.; Zhou, Y.; Sang, Y.Q.; Huang, H.; Zhang, J.S.; Meng, P.; Cai, L.L. Modeling the response of negative air ions to environmental factors using multiple linear regression and random forest. *Ecol. Inform.* **2021**, *66*, 101464. [CrossRef]
19. Huang, H.; Qian, C. Modeling PM2.5 forecast using a self-weighted ensemble GRU network: Method optimization and evaluation. *Ecol. Indic.* **2023**, *156*, 111138. [CrossRef]
20. Zhang, C.; Wu, Z.; Li, Z.; Li, H.; Lin, J. Inhibition effect of negative air ions on adsorption between volatile organic compounds and environmental particulate matter. *Langmuir ACS J. Surfaces Colloids* **2020**, *36*, 5078–5083. [CrossRef]
21. Lu, Z.; Wei, Z.; Li, Q.; Wang, H. Numerical Simulation of Dust Deposition in the Filter Tube of Adsorption Air Purifier. *Math. Probl. Eng.* **2019**, *2019*, 9478659. [CrossRef]
22. Avila, B.S.; Mendoza, D.P.; Ramírez, A.; Peñuela, G.A. Occurrence and distribution of persistent organic pollutants (POPs) in the atmosphere of the Andean city of Medellin, Colombia. *Chemosphere* **2022**, *307*, 135648. [CrossRef] [PubMed]
23. Henríquez, C.; Romero, H. *Urban Climates in Latin America*; Springer: Gewerbestrasse, Switzerland, 2019.
24. Shamila, C.; Sukhdev, K.; Rohit, P.; Baburaj, P. Experimental Validation of Mathematical Modeling of MoX Sensors. In Proceedings of the 2024 International Conference on Advancements in Power, Communication and Intelligent Systems (APCI), Kannur, India, 21–22 June 2024; pp. 1–5.
25. Wang, Y.; Wang, H.; Chang, S.; Avram, A. Prediction of daily pm 2.5 concentration in china using partial differential equations. *PLoS ONE* **2018**, *13*, e0197666. [CrossRef] [PubMed]
26. Keil, C. A tiered approach to deterministic models for indoor air exposures. *Appl. Occup. Environ. Hyg.* **2000**, *15*, 145–151. [CrossRef] [PubMed]
27. Babu Saheer, L.; Bhasy, A.; Maktabdar, M.; Zarrin, J. Data-driven framework for understanding and predicting air quality in urban areas. *Front. Big Data* **2022**, *5*, 822573. [CrossRef] [PubMed]
28. Yang, F.; Huang, G. An optimized decomposition integration model for deterministic and probabilistic air pollutant concentration prediction considering influencing factors. *Atmos. Pollut. Res.* **2024**, *15*, 102144. [CrossRef]
29. Ortiz-Grisales, P.; Patiño-Murillo, J.; Duque-Grisales, E. Comparative study of computational models for reducing air pollution through the generation of negative ions. *Sustainability* **2021**, *13*, 7197. [CrossRef]
30. Dalmau, M.; Atanasova, N.; Gabarrón, S.; Rodriguez-Roda, I.; Comas, J. Comparison of a deterministic and a data driven model to describe MBR fouling. *Chem. Eng. J.* **2015**, *260*, 300–308. [CrossRef]
31. Kundu, G.K.; Kundu, A.; Kundu, A. Mass of System as a function of Energy. *Asian J. Basic Sci. Res.* **2023**, *5*, 48–53. [CrossRef]
32. Whitaker, R.D. An historical note on the conservation of mass. *J. Chem. Educ.* **1975**, *52*, 658. [CrossRef]
33. Chakraborty, M.; Bansal, S.; Masiwal, R.; Awasthi, A. 5 Air-Pollution Modelling Aspects: An Overview. In *Air Pollution: Sources, Impacts and Controls*; CABI: London, UK, 2019; pp. 79–95.
34. Fantke, P.; Jolliet, O.; Apte, J.S.; Hodas, N.; Evans, J.; Weschler, C.J.; Stylianou, K.S.; Jantunen, M.; McKone, T.E. Characterizing aggregated exposure to primary particulate matter: Recommended intake fractions for indoor and outdoor sources. *Environ. Sci. Technol.* **2017**, *51*, 9089–9100. [CrossRef] [PubMed]
35. Wang, J.; Li, Z.; Liang, X.; Zhang, H.; Ou, Y. PM2.5 removal by negative ions and the effects of temperature humidity and negative-ion concentration. *Fresenius Environ. Bull.* **2021**, *30*, 5844–5854.
36. Zauner-Wieczorek, M.; Curtius, J.; Kürten, A. The ion–ion recombination coefficient α: Comparison of temperature-and pressure-dependent parameterisations for the troposphere and stratosphere. *Atmos. Chem. Phys.* **2022**, *22*, 12443–12465. [CrossRef]

37. Gao, T.; Liu, F.; Wang, Y.; Mu, S.; Qiu, L. Reduction of atmospheric suspended particulate matter concentration and influencing factors of green space in urban forest park. *Forests* **2020**, *11*, 950. [CrossRef]
38. Wendt, E.A.; Quinn, C.; L'Orange, C.; Miller-Lionberg, D.D.; Ford, B.; Pierce, J.R.; Mehaffy, J.; Cheeseman, M.; Jathar, S.H.; Hagan, D.H.; et al. A low-cost monitor for simultaneous measurement of fine particulate matter and aerosol optical depth–Part 3: Automation and design improvements. *Atmos. Meas. Tech.* **2021**, *14*, 6023–6038. [CrossRef]
39. Jayaratne, R.; Liu, X.; Ahn, K.H.; Asumadu-Sakyi, A.; Fisher, G.; Gao, J.; Mabon, A.; Mazaheri, M.; Mullins, B.; Nyaku, M.; et al. Low-cost PM2.5 sensors: An assessment of their suitability for various applications. *Aerosol Air Qual. Res.* **2020**, *20*, 520–532.
40. Orejas, J.; Pfeuffer, K.P.; Ray, S.J.; Pisonero, J.; Sanz-Medel, A.; Hieftje, G.M. Effect of internal and external conditions on ionization processes in the FAPA ambient desorption/ionization source. *Anal. Bioanal. Chem.* **2014**, *406*, 7511–7521. [CrossRef] [PubMed]
41. An, Y.; Su, M.; Hu, Y.; Hu, S.; Huang, T.; He, B.; Yang, M.; Yin, K.; Lin, Y. The influence of humidity on electron transport parameters and insulation performance of air. *Front. Energy Res.* **2022**, *9*, 806595. [CrossRef]
42. Ortiz-Grisales, P.M.; Gutiérrez-León, L.; Zuluaga-Ríos, C.D. Influence of Temperature Variability on the Efficacy of Negative Ions in Removing Particulate Matter and Pollutants: An Experimental Database. *Data* **2024**, *9*, 131. [CrossRef]
43. Marulanda-Durango, J.; Zuluaga-Ríos, C. A meta-heuristic optimization-based method for parameter estimation of an electric arc furnace model. *Results Eng.* **2023**, *17*, 100850. [CrossRef]
44. Price, K. *Differential Evolution: A Practical Approach to Global Optimization*; Springer Science & Business Media: Berlin/Heidelberg, Germany, 2006.
45. Teng, Y.; Huang, X.; Ye, S.; Li, Y. Prediction of particulate matter concentration in Chengdu based on improved differential evolution algorithm and BP neural network model. In Proceedings of the 2018 IEEE 3rd International Conference on Cloud Computing and Big Data Analysis (ICCCBDA), Chengdu, China, 20–22 April 2018; pp. 100–106.
46. Kumar, D. Evolving Differential evolution method with random forest for prediction of Air Pollution. *Procedia Comput. Sci.* **2018**, *132*, 824–833.
47. Wu, Y.Y.; Chen, Y.C.; Yu, K.P.; Chen, Y.P.; Shih, H.C. Deposition removal of monodisperse and polydisperse submicron particles by a negative air ionizer. *Aerosol Air Qual. Res.* **2015**, *15*, 994–1007. [CrossRef]
48. Yu, K.P. Enhancement of the deposition of ultrafine secondary organic aerosols by the negative air ion and the effect of relative humidity. *J. Air Waste Manag. Assoc.* **2012**, *62*, 1296–1304. [CrossRef] [PubMed]
49. Yu, K.P.; Lin, C.C.; Yang, S.C.; Zhao, P. Enhancement effect of relative humidity on the formation and regional respiratory deposition of secondary organic aerosol. *J. Hazard. Mater.* **2011**, *191*, 94–102. [CrossRef]
50. Yu, K.P.; Lee, W.M.G.; Peng, C.J.; Chen, Y.C.; Shen, W.T. Effects of roughness, dielectric constant and electrical resistivity of wall on deposition of submicron particles driven by ionic air purifier. *J. Environ. Chem. Eng.* **2017**, *5*, 3108–3114. [CrossRef]
51. Yu, K.P.; Shih, H.C.; Chen, Y.C.; Yang, X.E. Effect of turbulence intensity and particle characteristics on the deposition of submicron particles enhanced by the ionic air purifier. *Build. Environ.* **2017**, *114*, 166–177. [CrossRef]
52. University of Central Florida. 18.5 Collision Theory and the Effect of Temperature on Reaction Rate. In *Chemistry Fundamentals*; UCF Pressbooks: Online Resource. Available online: https://pressbooks.online.ucf.edu/chemistryfundamentals/chapter/collision-theory/ (accessed on 24 December 2024).
53. Zhang, L.; Ou, C.; Magana-Arachchi, D.; Vithanage, M.; Vanka, K.S.; Palanisami, T.; Masakorala, K.; Wijesekara, H.; Yan, Y.; Bolan, N.; et al. Indoor particulate matter in urban households: Sources, pathways, characteristics, health effects, and exposure mitigation. *Int. J. Environ. Res. Public Health* **2021**, *18*, 11055. [CrossRef]
54. Li, T.; Yu, Y.; Sun, Z.; Duan, J. A comprehensive understanding of ambient particulate matter and its components on the adverse health effects based from epidemiological and laboratory evidence. *Part. Fibre Toxicol.* **2022**, *19*, 67. [CrossRef] [PubMed]
55. Wang, S.; Ren, Y.; Xia, B.; Liu, K.; Li, H. Prediction of atmospheric pollutants in urban environment based on coupled deep learning model and sensitivity analysis. *Chemosphere* **2023**, *331*, 138830. [CrossRef] [PubMed]
56. García-Moreno, A.; González-Barbosa, J.; Hurtado-Ramos, J.; Ornelas-Rodríguez, F.; Ramírez-Pedraza, A. Análisis de la sensibilidad en un modelo de calibración cámara-LiDAR. *Rev. Int. Métodos Numéricos Para Cálculo Diseño Ing.* **2016**, *32*, 193–203. [CrossRef]
57. Ribeiro, L.S.; de Miranda, G.B.; Chapiro, G.; dos Santos, R.W.; Rocha, B.M. A workflow for uncertainty quantification of numerical models for foam-based EOR. In Proceedings of the Rio Oil & Gas Expo and Conference, Rio de Janeiro, Brazil, 26–29 September 2022.
58. Bose, A.; Chowdhury, I.R. Towards cleaner air in Siliguri: A comprehensive study of PM2.5 and PM10 through advance computational forecasting models for effective environmental interventions. *Atmos. Pollut. Res.* **2024**, *15*, 101976. [CrossRef]